EFFECT OF SHOT PEENING ON FINE GRAIN STEEL

K. Seki 1, M. Hashimoto 2, M. Gotoh 3, H. Hirose 4

1 Kanazawa University, Kakumamachi, Kanazawa, Ishikawa 920-1164, Japan
2 Hashimoto Eng. Consultant Office, 234-2 Yokonemachi, Ohbu, Aichi 474-0011, Japan
3 Kanazawa University, Kakumamachi, Kanazawa, Ishikawa 920-1164, Japan
4 Kinjo University, 1200 Kasamamachi, Hakusan, Ishikawa 924-8511, Japan

ABSTRACT

Recently, the improvement of the high strength of fine grain steels has been investigated actively. In the present study, interior and surface residual stress distributions in fine grain steel after shot peening were measured by X-ray diffraction. Moreover, the hardening effect near the shot peened surface was also examined. The relationships between the hardening effects of shot peening and the grain size of material are discussed. It is found that both the initial hardness before shot peening and the mean grain size of the sample had an influence on the distributions of the hardness and the residual stress.

KEY WORDS

Fine Grain Steel, X-ray, Residual Stress, FWHM, Hardness

INTRODUCTION

Recently, fine grain steels have been investigated actively (N. Tsuji, 2002 ; M. Niikura, 2003) to achieve high strength. Various methods such as equal-channel angular pressing (R. Z. Valiev, N. A. Krasilnkov and N. K. Tsenev, 1991) and accumulative roll-bonding (Y. Saito, N. Tsuji, H. Utsunomiya *et al*.,1998) have been devised to form fine grains, which are generally produced by applying high strain alone. These methods yield excellent materials with different characteristics and recyclability. Moreover, fine grain steels have high yield stress, as expected by the Hall－Petch relationship. Therefore, these materials are considered for use as structural material.

Welding (T. Otani and K. Sasabe, 2003) is one of the most effective methods for connecting structural components. Nevertheless, the negative influence of tensile residual stresses and coarse grains due to the welding process must be taken into consideration. It has been proved that the shot peening process can effectively overcome these problems. Change in the state of material caused by shot peening is reported by O. Vöhringer (O. Vöhringer, 1987). However, the confirmation of the same tendency in fine grain steel is not yet confirmed. In this study, samples prepared with various mean grain sizes were processed by shot peening. The residual stress distribution after shot peening was measured by X-ray diffraction. Moreover, the distribution of the hardening effect near the shot peened surface was observed. The relationships between the effects of shot peening and the grain size of material are discussed.

EXPERIMENTAL PROCEDURE

Specimens

In this study, JIS SM490 and Nakayama Fine Grain 600 (NFG600) steels (It was made by Nakayama steel works, LTD. in Japan) were used. The chemical compositions of SM490 and NFG600 are shown in Table I, and their mechanical properties are shown in Table II. Moreover, NFG600 was annealed by two processes to examine the influence of the grain size and to obtain the same hardness as SM490; one was maintained at 1073 K for one hour (in an atmospheric furnace) and the other was maintained for two hours at 1423 K.

These specimens were cut out to the size of 30 × 30 ×10 mm size. Then, the influence of the rolling process was removed by grinding the sample surface by 2mm, followed by electropolishing until the residual stress in the samples was removed.

Table I. Chemical compositions (wt.%).

	C	Si	Mn	P	S
SM490	0.16	0.25	1.60	0.018	0.005
NFG600	0.17	0.36	1.30	0.011	0.007

Table II. Mechanical properties.

	Yield stress, MPa	Tensile strength, MPa	Elongation, %
SM490	358	543	25
NFG600	461	602	30

Shot peening process

The conditions during the shot peening process are shown in Table III. The residual stress on the surface of the material was removed by electropolishing before shot peening (K. Iida and K. Tosha, 1986; K. Iida and K. Tosha, 1988). Both the mean grain size and initial hardness of all specimens are shown in Table IV.

Table III. Conditions of Shot-Peening process.

	I	II	III	IV
Peening machine	Air type			
Shot peening material (Hardness)	BPS150 (HV 250)		RCW06AC (HV150)	
Peening time, sec	15	60	20	120
Arc height, mmA	0.03	0.08	0.02	0.39
Distance, mm	100			
Nozzle diameter, mm	ϕ9.0			

Table IV. Initial mean grain size and hardness of each specimen.

	Initial grain size (μm)	Initial hardness (HV)
SM490	16	155
NFG600	3	185
NFG600 Annealing (Annealing temperature: 1073 K)	6	163
NFG600 Annealing (Annealing temperature: 1423 K)	45	130

Hardness test.

Shot peening modifies the hardness below the surface. The distribution of Vickers hardness was measured by a micro−Vickers hardness tester at the cross section in a depth of 20 μm and more. However, the surface of the specimens was examined in vertical view.

Conditions of X-ray stress measurement.

X-ray diffraction was used to measure the residual stress. Samples were measured by the $\sin^2\psi$ method. The measurement conditions are shown in Table V. However, the X-ray stress measurement yields only the plane stress. The residual stress was measured for each fresh surface. Electropolishing was performed in a phosphoric acid solution. The parameters of our measurement are shown in Eq. (1).

Table V. Conditions of stress measurement.

Characteristic radiation	Cr-Kα
Tube voltage, kV	30
Tube Current, mA	10
Kβ filter	V
Diffraction plane	211
Diffraction angle 2θ, deg	156.41

$$\sigma_x = -\frac{E_x}{2(1+\nu_x)} \cdot \cot\theta_0 \cdot \frac{\pi}{180} \cdot \frac{\partial(2\theta_\psi)}{\partial(\sin^2\psi)} \quad \text{(MPa)} \qquad (1)$$

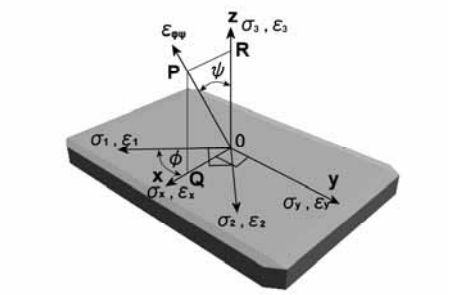

Fig.1 Coordinates of X-ray stress measurement.

RESULTS AND DISCUSSION

The layer influenced by shot peening could not be observed for shot peening conditions I and III. By contrast, the influenced layer by shot peening was observed at 20μm from the surface for shot peening conditions II and IV (Fig. 2 and Fig. 3). For this reason, it is possible to think which acute change occurs to the distribution of X-ray full width of half maximum intensity (FWHM), the residual stress and the hardness, respectively.

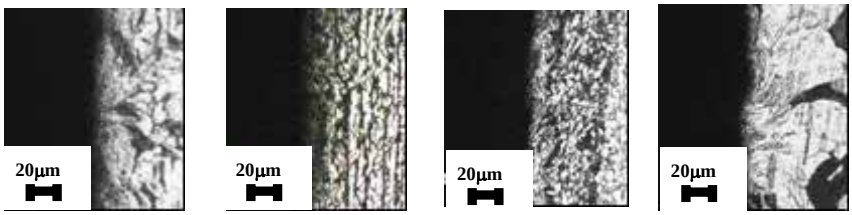

SM490 NFG600 NFG600 (1073K) NFG600 (1423K)

Fig. 2. Microstructures in a section after shot peening (Shot peening condition II).

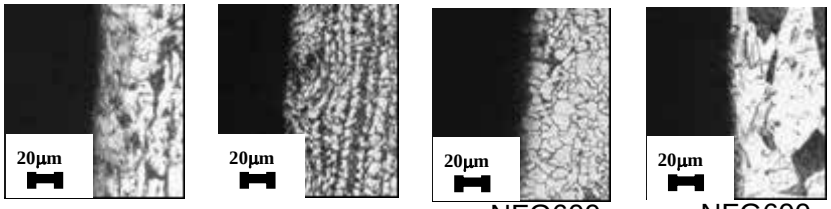

Fig. 3 Microstructures in a section after shot peening (Shot peening condition IV).

Figure 4 shows the Vickers hardness distribution. The larger the mean grain size, the steeper the slope of the hardness distribution near the surface. However, high values of hardness were not observed for the nanocrystal layer, because of its thinness. In addition, the depth influence by shot peening depended on the initial hardness.

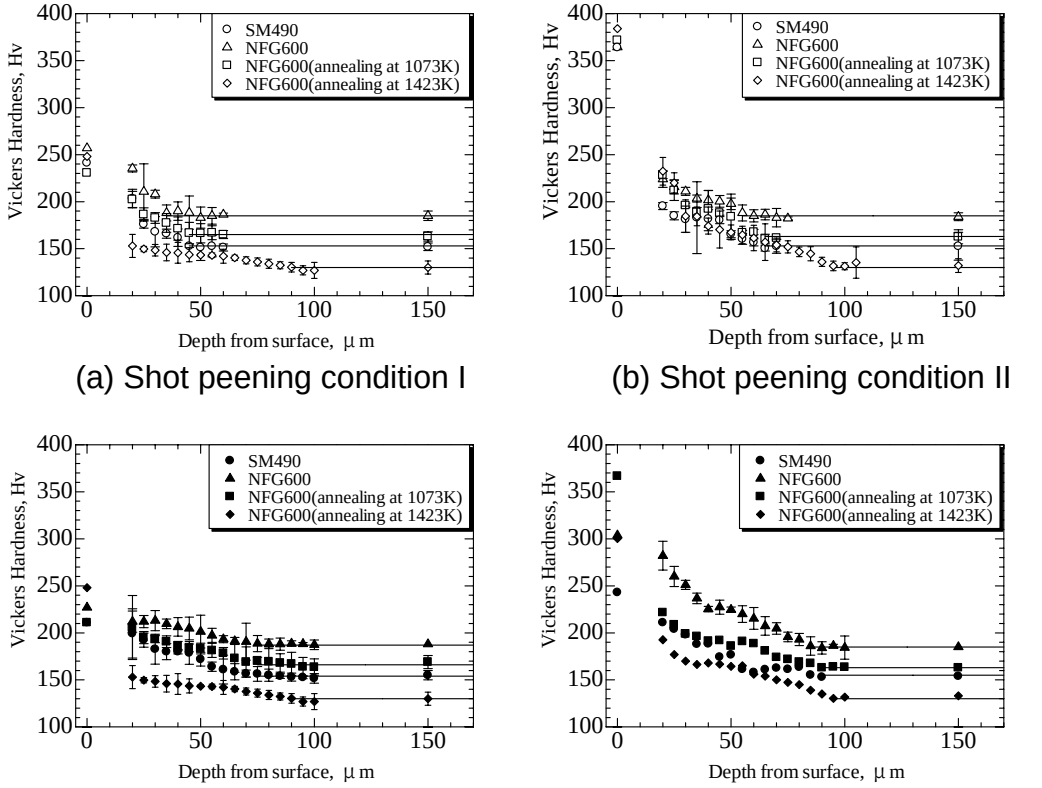

(a) Shot peening condition I (b) Shot peening condition II

(c) Shot peening condition III (d) Shot peening condition IV

Fig. 4. Vickers hardness distribution.

The result of FWHM distribution versus depth is shown in Fig. 5. FWHM is a parameter that shows changes in particle size and root-mean-squared strain $<\varepsilon^2>^{1/2}$ caused by plastic deformation. In this study, FWHM is normalized by the condition without processing.

Similar to the case of the hardness distribution, an abrupt change was observed near the surface. In addition, an abrupt change related to the mean grain size was confirmed.

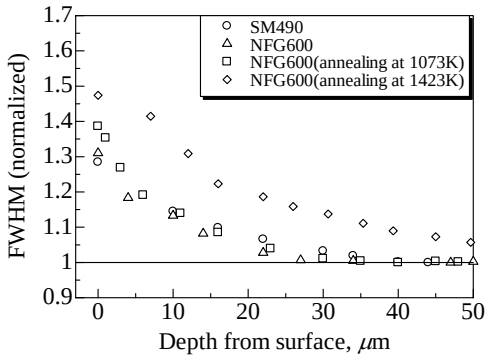

(a) Shot peening condition I

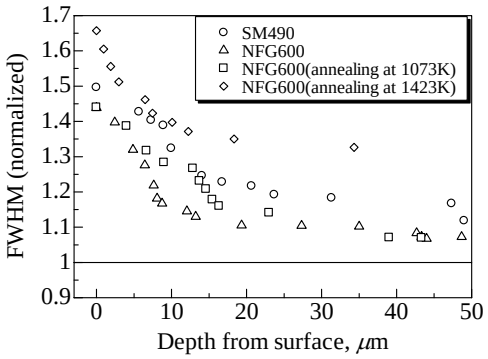

(b) Shot peening condition II

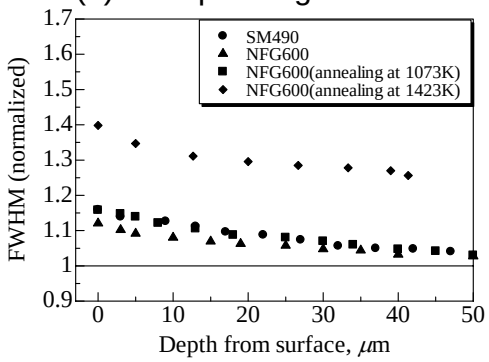

(c) Shot peening condition III

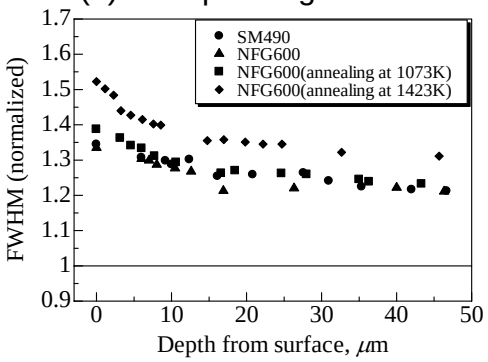

(d) Shot peening condition IV

Fig. 5. FWHM distribution.

Figure 6 shows the residual stress distribution. High compressive stress was observed at 50μm depth in every condition except condition I. The depth where residual stress becomes zero was deeper than the depth where FWHM became steady due to plastic constraint.

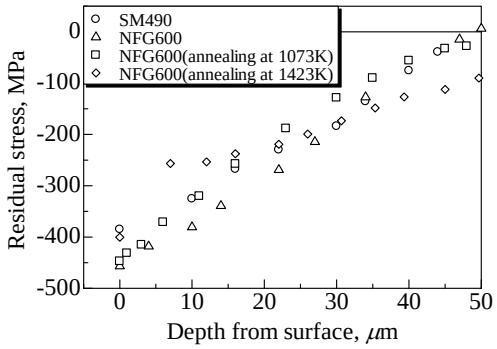

(a) Shot peening condition I

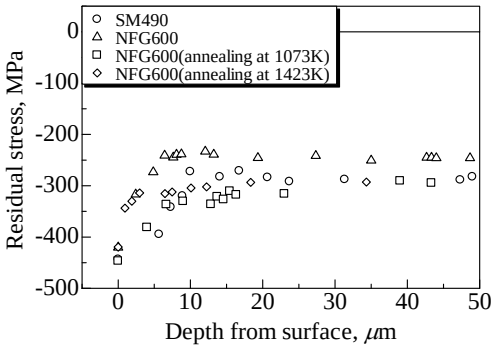

(b) Shot peening condition II

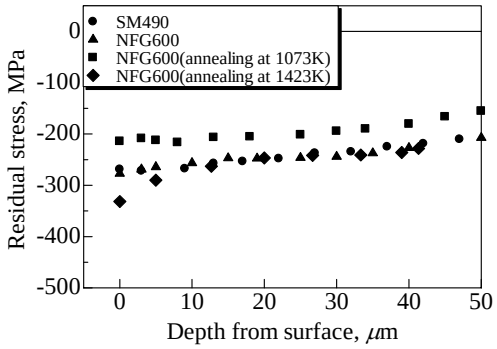

(c) Shot peening condition III

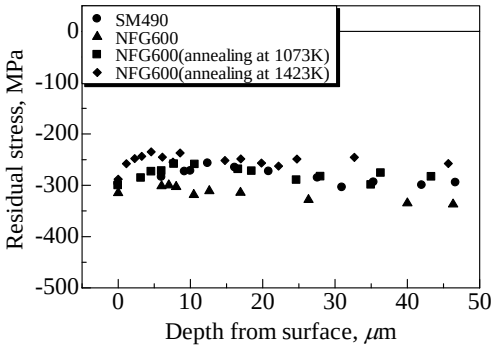

(d) Shot peening condition IV

Fig. 6. Residual stress distribution.

In the condition I, the depth where residual stress became zero was shallower than 50μm. In the condition III, the depth (where residual stress become zero) was over 50μm. On the other hand, comparing the condition II with IV, the change of residual stress was larger in condition II as far as the surface was concerned. The residual stress also became steady at the greater depth.

It finds that the work-hardening exponent increases with the mean grain size according to Eq.(2).

$$n = (1/k)^{\gamma} d^{\gamma/2} \quad (2)$$

Here,
n is the work-hardening exponent;
d is the mean grain size; and
k and *γ* are the material constants

Eq.(2) explains that *n* depends on *d*. Therefore, as *d* increases, the hardness near the surface increase.

Both FWHM and residual stress can change abruptly versus depth as mentioned above. However, this tendency is less certain in residual stress (condition I and III). This is attributed to the stress gradient in X-ray penetration depth.

CONCLUSION

(1) In the influence of the mean grain size, FWHM and the hardness show an abrupt change at less than 20μm depth.
(2) Steel with the grain size of over 3μm could have done surface reforming without deteriorating.
(3) The convergence depth on the behavior between FWHM and residual stress near the surface is different. It is caused by the stress gradient within X-ray penetration depth.

REFERENCES

K. Iida and K. Tosya: Journal of the Japan Society of Precision Engineering Vol. 52 (1986), pp. 535-539.

K. Iida and K. Tosya: Journal of the Japan Society of Precision Engineering Vol. 54 (1988), pp. 107-111.

M. Niikura: Bulletin of the Iron and Steel Institute of Japan Vol. 8 (2003), pp. 718-724.

N. Tsuji: The journal of the Iron and Steel Institute of Japan Vol. 88 (2002), pp. 359-369.

O. Vöhringer: ICSP3(1987), pp185-204.

R. Z. Valiev, N. A. Krasilnikov and N. K. Tsenev: Materials Science and Engineering A, Vol. 137 (1991), pp. 35-40.

T. Otani and K. Sasabe: Quarterly journal of the Japan Welding Society Vol. 21 (2003), pp. 243-248.

Y. Saito, N. Tsuji, H. Utsunomiya and et al: Scripta Materialia 39 (9), pp. 1221-1227.